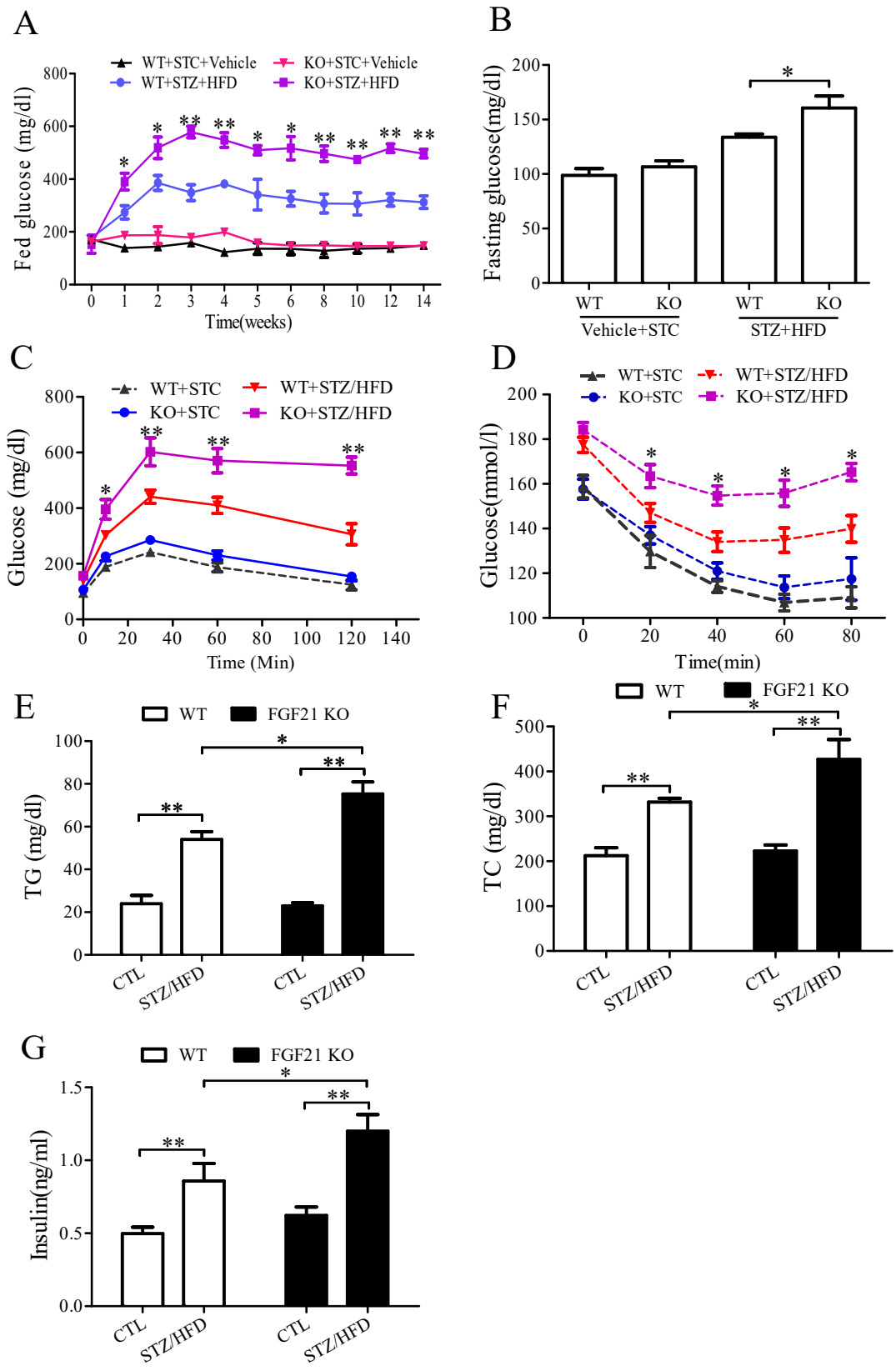

Supplemental Fig. 1 FGF21 deletion impairs glucose tolerance in STZ/HFD-induced diabetic mice. (A) Fed glucose levels in KO and WT mice treated with STZ/HFD or vehicle. (B) Fasting glucose levels at 16 weeks after treatment with STZ/HFD treatment. (C) GTT and (D) ITT were performed at 14-15 weeks after STZ treatment. (E-G) Serum triglycerides, total cholesterol and insulin levels at 16 weeks after treatment with STZ. Data are presented as mean±SEM. *, $p<0.05$; **, $p<0.01$. n=6-7 in each group.

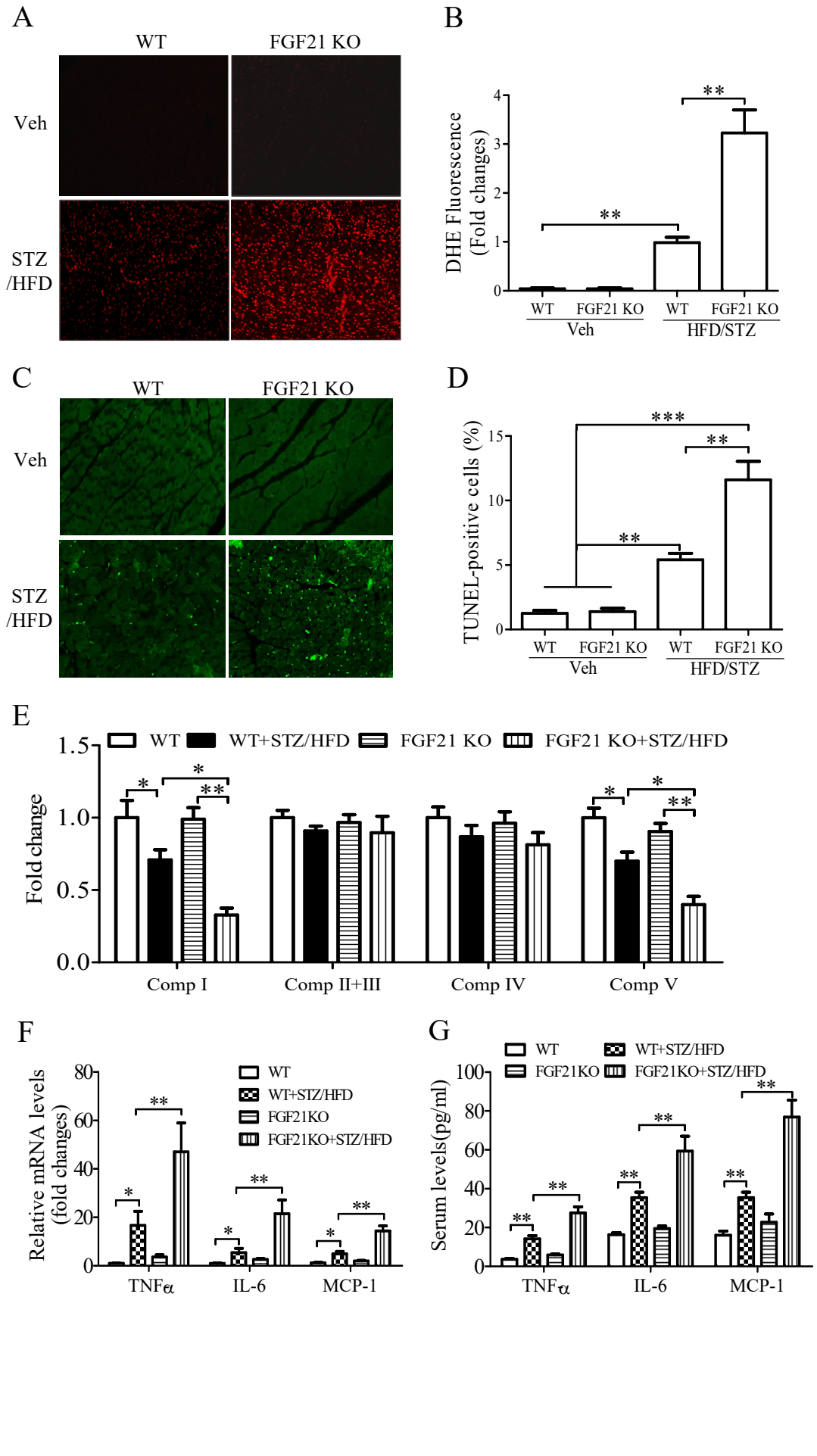
A
WT
FGF21 KO
Veh
STZ
/HFD
B
DHE Fluorescence
(Fold changes)
WT
FGF21 KO
WT
FGF21 KO
Veh
HFD/STZ
C
WT
FGF21 KO
Veh
STZ
/HFD
D
TUNEL-positive cells (%)
WT
FGF21 KO
WT
FGF21 KO
Veh
HFD/STZ
E
WT
WT+STZ/HFD
FGF21 KO
FGF21 KO+STZ/HFD
Fold change
Comp I
Comp II+III
Comp IV
Comp V
F
Relative mRNA levels
(fold changes)
WT
WT+STZ/HFD
FGF21KO
FGF21KO+STZ/HFD
TNFα
IL-6
MCP-1
G
WT
WT+STZ/HFD
FGF21KO
FGF21KO+STZ/HFD
Serum levels(pg/ml)
TNFα
IL-6
MCP-1

Supplementary Fig. 2 FGF21 deficiency augments cardiac oxidative stress and mitochondrial dysfunction in STZ/HFD-induced diabetic mice. (A) Representative imaging of ROS levels tested by DHE staing. (B) Intercellular ROS levels in Cardiac sections collected in Fig.2 (amplify × 200). (C) Representative imaging of cardiomyocytes apoptosis tested by TUNEL. (D) Results of cardiomyocytes apoptosis in cardiac section (amplify × 200). (E) The activities of MRC complex I, II+III, IV and V in cardiac tissues collected in Fig.2. (F) Cardiac mRNA levels of local inflammatory factors including TNF-α, IL-6 and MCP-1 measured by real-time qPCR. (G) Circulating levels of inflammatory factors including TNF-α, IL-6 and MCP-1. Data are presented as mean ± SEM. *, $p<0.05$; **, $p<0.01$. n= 6-7 in each group.

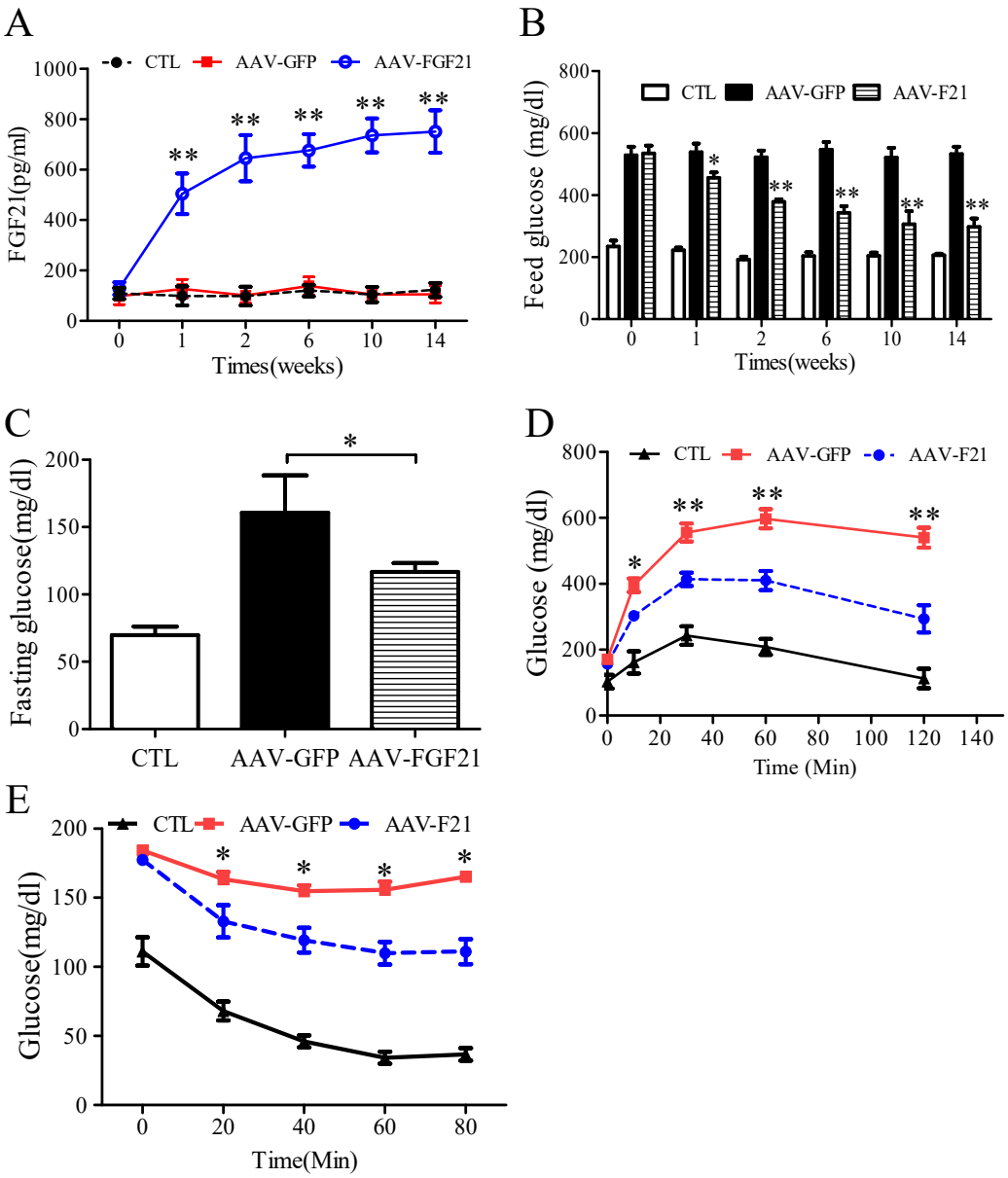

Supplemental Fig. 3. **Overexpression of FGF21 improves abnormal glucose tolerance in STZ/HFD-treated mice.** 8-week old FGF21 KO male mice were injected intraperitoneally by a single dosage of 100mg/kg STZ after feeding with 4 weeks HFD, and then intravenously injected with 1×10^{12} genomic particles of adeno-associated virus (AAV) encoding FGF21, or GFP. blood glucose and FGF21 levels were examined at 1, 2, 6, 10 and 14 weeks, Glucose and insulin tolerance tests were performed at 15 weeks, after treatment with AAV-FGF21 or AAV-GFP. FGF21 KO male mice with standard chow diet were used as a control. (A) Circulating FGF21 levels and (B) Feed glucose levels in STZ/HFD-treated mice infected with AAV-FGF21, or with AAV-GFP as well as FGF21 KO mice with standard chow diet as control. (C) Fasting glucose levels at 16 weeks before scarification. (D) GTT performed at 14 weeks after infection with AAV-FGF21 or AAV-GFP. (E) ITT performed at 15 weeks after infection with AAV-FGF21 or AAV-GFP. Data are presented as mean±SEM. *, $p<0.05$; **, $p<0.01$. n=6 in each group.

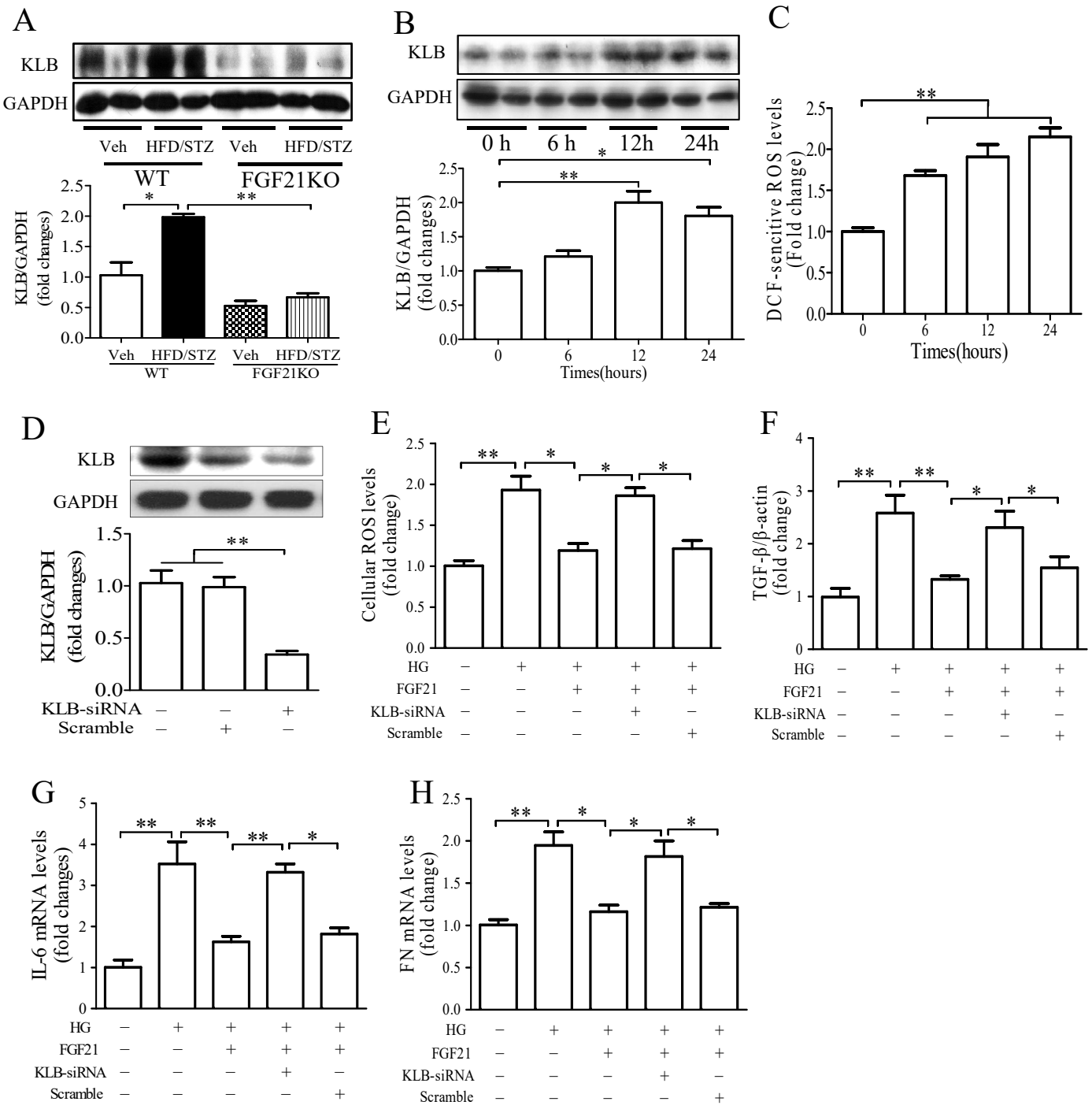

Supplemental Fig. 4. **The protective effects of FGF21 against glucose-induced cytotoxicity is abrogated by genetic inhibition of β-klotho in cardiomyocytes.** (A) Immunoblot analysis for β-klotho (KLB) expression in cardiac tissues collected in Fig. 2. (B,C) Primary mouse cardiomyocytes were treated with HG (33mM) for different time-point, and cellular PON1 expression (B) was measured by immunoblot analysis, and intracellular ROS products (C) were tested by DCFH-DA assay as described in *Methods*. (D-F) Primary mouse cardiomyocytes were infected with β-klotho siRNA or scrambled RNA for 36 h, and then incubated with HG for 6 h, followed by treatment with rmFGF21 (50ng/ml) or vehicle for 24 hours. (D) Immunoblot analysis for the expression levels of KLB in cardiomyocytes after infection with KLB-siRNA or scramble. (E) The intracellular ROS levels measured at 24 hours after treatment with FGF21. The mRNA expression levels of TGF-β (F), fibronectin (G) and IL-6 (H) were measured by real-time qPCR. Data are presented as mean±SEM. *, $p<0.05$; **, $p<0.01$. All in vitro data were obtained from at least 5 independent experiments.

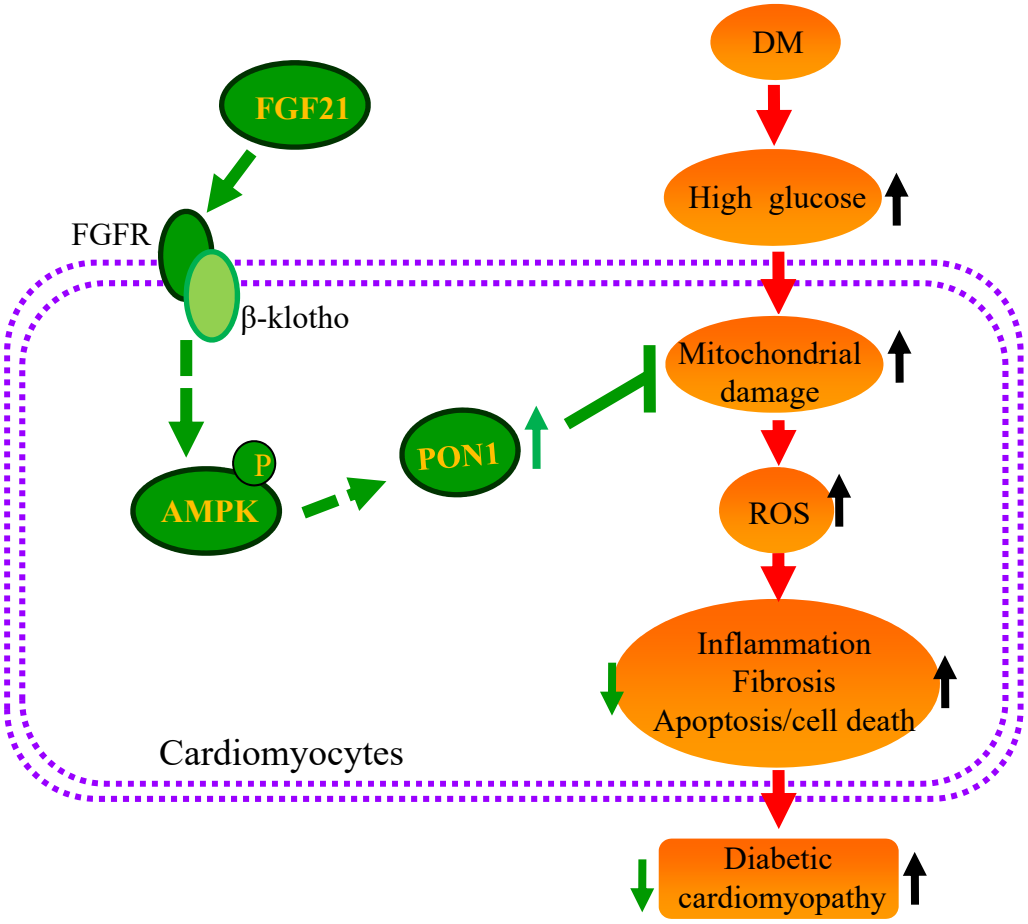

Supplemental Fig. 5 A proposal model by which FGF21 protects against diabetic cardiomyopathy in mice. High circulating levels of glucose in diabetic mice triggers oxidative stress and accelerates mitochondria damage, resulting in elevated inflammation, fibrosis and cell death, consequently leads to aggravate diabetic cardiomyopathy. FGF21 activates AMPK activation, and then enhances PON1 expression, which in turn inhibits HG-induced oxidative stress, and contributes to improved mitochondrial dysfunction, inhibits local inflammation, fibrosis and cardiomyocyte apoptosis, thereby prevents from diabetic cardiomyopathy.